Northern Bering Sea tip jets

G. W. K. Moore[1] and R. S. Pickart[2]

Received 28 February 2012; revised 27 March 2012; accepted 28 March 2012; published 28 April 2012.

[1] Low-level regions of high wind speed known as tip jets have been identified near Cape Farewell, Greenland's southernmost point. These wind systems contribute to this area being the windiest location on the ocean's surface and play an important role in the regional weather and climate. Here we present the first analysis of the wind systems that make the Siberian coast of the northern Bering Sea the windiest location in the North Pacific Ocean during the boreal winter. In particular we show that tips jets characterized by enhanced northeasterly winds occur in the vicinity of the two prominent headlands along the coast, Cape Navarin and Cape Olyutorsky. The advance of sea ice in the region is shown to impact the frequency and location of the high speed winds in the vicinity of these two capes. Furthermore, we show that these jets are associated with the interaction of extra-tropical cyclones with the high topography of the Koryak Mountain range, situated just inland of the capes. The windstress imparted to the ocean via the tip jets is argued to help drive the formation of dense water in winter in the northern Bering Sea, thus playing an important role in the regional oceanic circulation. **Citation:** Moore, G. W. K., and R. S. Pickart (2012), Northern Bering Sea tip jets, *Geophys. Res. Lett.*, *39*, L08807, doi:10.1029/2012GL051537.

1. Introduction

[2] A global climatology of the surface marine wind field has confirmed that the flow distortion associated with coastal mountain ranges is responsible for many examples of high surface winds around the globe [*Sampe and Xie*, 2007]. The windiest location in the world ocean is situated near Cape Farewell, the southernmost tip of Greenland, and is the result of the interaction of extra-tropical cyclones with the high topography of the region. This results in the formation of intense surface wind systems known as tip jets that can be either easterly or westerly in character [*Doyle and Shapiro*, 1999; *Moore*, 2003]. The dynamics of these two classes of Cape Farewell tip jets are very different: the westerly jets are the result of Bernoulli acceleration down the lee slope [*Doyle and Shapiro*, 1999] as well as acceleration around Cape Farewell [*Moore and Renfrew*, 2005; *Våge et al.*, 2009]. In contrast, the easterly tip jets appear to be the result of barrier flow undergoing an adjustment process resulting from the removal of the topographic barrier [*Moore and Renfrew*, 2005; *Outten et al.*, 2009]. Cross-isobar acceleration resulting from the deceleration of the flow impinging on the topographic barrier also contributes to easterly tip jet formation [*Renfrew et al.*, 2009a]. In this sense, easterly Cape Farewell tip jets are examples of so-called "corner jets" [*Barstad and Gronas*, 2005]. In addition to their regional impact on the weather and climate of southern Greenland, these wind events have also been proposed to have a dramatic impact on both the surface and deep ocean circulation in the region [*Doyle and Shapiro*, 1999; *Pickart et al.*, 2003; *Haine et al.*, 2009].

[3] *Sampe and Xie* [2007] identified other regions where high surface wind speeds are associated with coastal topography. After southern Greenland, the windiest location during the boreal winter is located along the Siberian coast of the northern Bering Sea (Figure S1 in the auxiliary material).[1] The coast has two prominent headlands, Capes Navarin and Olyutorsky. Just inland of the coast are the Koryak Mountains, an extension of the Kamchatka Mountain range. Elevations within the range are on the order of 1000 m or higher, with the highest mountain in the range being Mount Ledyakaya with an elevation of 2400 m (Figure S1). The high winds in this region are a hazard to marine traffic, with one of the deadliest shipping losses in the Bering Sea occurring near Cape Navarin in December 1999 when the Japanese vessel Anyo Maru sank in 20 m/s winds [*New York Times*, 1999].

[4] The Bering Sea is one of the world's most productive marine ecosystems [*Highsmith and Coyle*, 1990], and the source of Pacific water that flows into Arctic Ocean occurs via the Bering Strait. One of the main northward pathways into the strait is the Anadyr Current, which flows through the Gulf of Andayr situated to the north of Cape Navarin (Figure S1). During winter, the northeasterly winds in the region result in the frequent formation of a polynya and sea-ice production along the northern coast of the Gulf of Andayr [*Cavalieri and Martin*, 1994]. The resulting densification of the surface water forms a watermass that downwells via Ekman forcing [*Wang et al.*, 2009]. This is one of the sources of Pacific winter water [e.g., *Muench et al.*, 1988] that is eventually transported northward through Bering Strait and ultimately ventilates the cold halocline of the western Arctic Ocean.

[5] The co-location of the high winds along this coast and the atmospherically-forced oceanic circulation that is of climatological and ecological importance raises the issue as to the coupling of the two. In this paper, we use the high-resolution North American Regional Reanalysis (NARR) to

[1]Department of Physics, University of Toronto, Toronto, Ontario, Canada.
[2]Department of Physical Oceanography, Woods Hole Oceanographic Institution, Woods Hole, Massachusetts, USA.

Corresponding Author: G. W. K. Moore, Department of Physics, University of Toronto, 60 St. George St., Toronto, ON M5S 1A7, Canada. (gwk.moore@utoronto.ca)

Copyright 2012 by the American Geophysical Union.
0094-8276/12/2012GL051537

[1]Auxiliary materials are available in the HTML. doi:10.1029/2012GL051537.

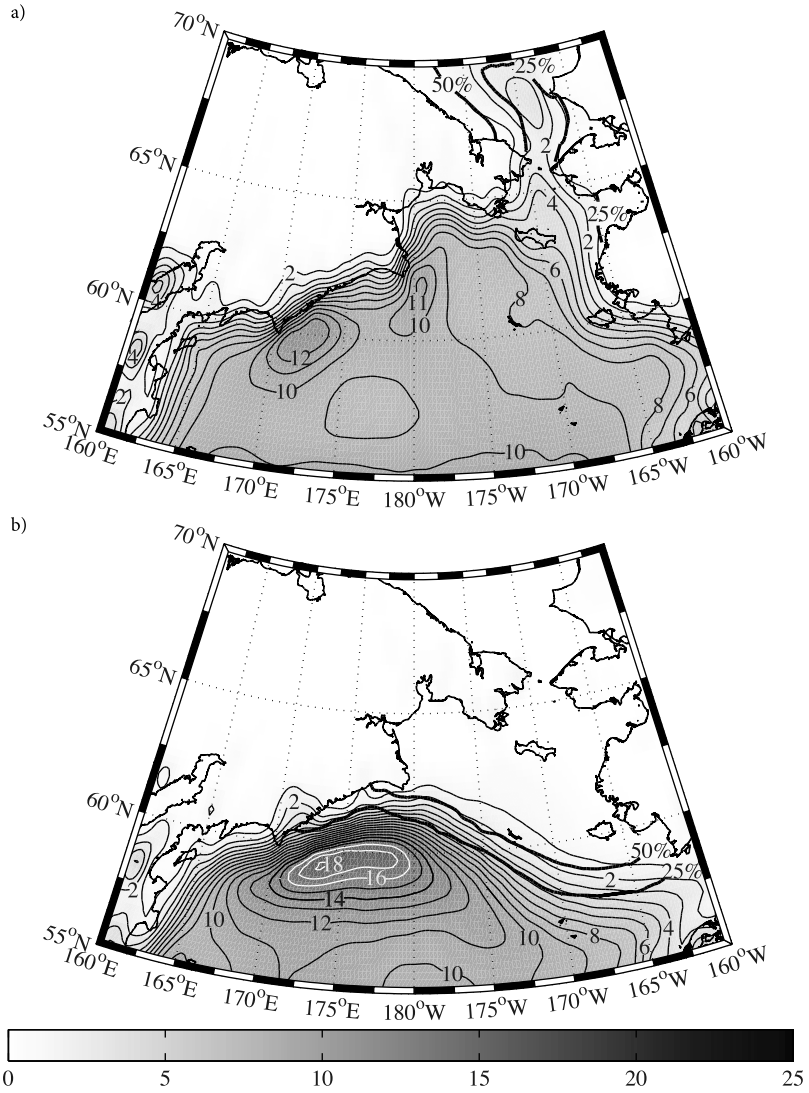

Figure 1. Frequency of occurrence of 10 m wind speeds in excess of 15 m/s (%- shading and thin lines) during: (a) November and (b) February from the NARR 1979-2011. Also shown by the thick lines are the monthly mean sea ice concentrations.

describe the atmospheric circulation patterns that result in the wind speed maximum along this coast.

2. Methods

[6] The NARR was created to provide a long-term consistent climate data set for North America [*Mesinger et al.*, 2006]. It uses the NCEP ETA model and its 3DVAR data assimilation system that includes direct assimilation of satellite radiances and precipitation, with lateral boundary conditions provided by the NCEP-2 global reanalysis. The model covers the North American continent and adjoining oceans including the northern Bering Sea. It has a horizontal resolution of approximately 32 km with 45 levels in the vertical of which 21 are below 850 mb. For this paper we use the full 3-hourly resolution data set for the period 1979–2011.

[7] Recent studies of the flow distortion around the topography of southern Greenland indicate that the NARR surface fields are in good overall agreement with both aircraft and buoy observations [*Moore et al.*, 2008; *Renfrew et al.*, 2009b]. In addition along the mountainous coast of California, the NARR has been shown to be able to capture the evolution of coastally trapped wind reversals [*Kanamaru and Kanamitsu*, 2007].

3. Results

[8] Using a similar approach as employed for the Cape Farewell region [*Moore*, 2003], we computed the frequency of occurrence of northerly high speed winds events in the northern Bering Sea during the months of November and February (Figure 1). In this instance, a cut-off of 15 m/s for the 10 m wind field was used to identify the high speed wind events. In November, there are two distinct maxima in the region that are situated in the vicinity of Cape Navarin and Cape Olyutorsky. A third maximum, with a much reduced frequency of occurrence, is situated in the southern Chukchi Sea just north of Bering Strait. There is also evidence of a modulation in the occurrence frequency in the vicinity of the two large islands, St Matthew and St Lawrence Islands, in the extreme northern Bering Sea. In contrast, a single maximum is identified in February that is situated in the vicinity of Cape Olyutorsky but farther offshore, by approximately 100 km, than the location of the corresponding maximum in

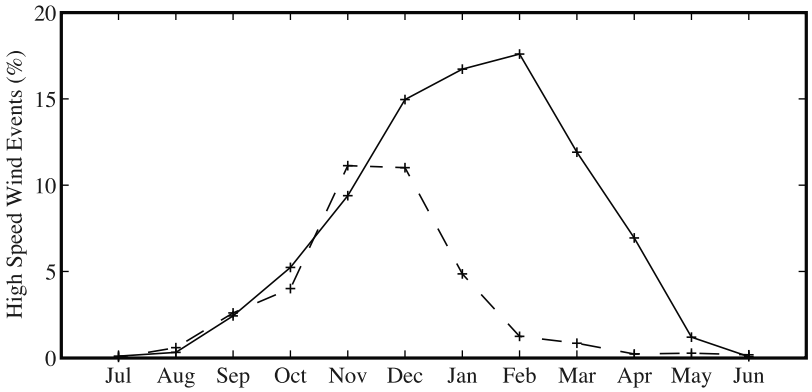

Figure 2. The annual cycle in the occurrence frequency of 10 m wind speeds in excess of 15 m/s at the Cape Olyutorsky site (solid line) and the Cape Navarin site (dashed line). Results based on the NARR 1979-2011.

November. In both months, an inland region of enhanced frequency of occurrence of high speed winds also exists just to the north of Cape Olyutorsky.

[9] Also shown in Figure 1 is the approximate edge of the sea ice, indicated by the 25% and 50% ice concentration contours. In November the ice edge is located in the southern Chukchi Sea. Note that the area of open water north of Bering Strait is co-located with the region of enhanced occurrence of high wind speed events. In February, by contrast, sea ice is present in the northern Bering Sea, covering the Cape Navarin region and extending down the coast towards Cape Olyutorsky. To the north of the ice edge, including the Cape Navarin region, there is a pronounced reduction in the frequency of high speed wind events.

[10] Details on the annual cycle in the frequency of occurrence of northerly high speed wind events in the region are shown in Figure 2. The Cape Navarin and Cape Olyutorsky sites are defined to be the locations of the relative maxima in their vicinity during November and February, respectively. At both sites there is a pronounced annual cycle with a low frequency of occurrence during the warm season and an elevated occurrence frequency during the cool season. At the Cape Navarin site, there is a maximum in November–December that is followed by a rapid decrease, with the occurrence frequency in January being 50% lower than those in the preceding two months. At the Cape Olyutorsky site, the occurrence frequency is a maximum in February, at levels that are 50% higher than the maximum at the Cape Navarin site. The subsequent dropoff is also not as pronounced as that at the more northern site. It should be noted that southerly high speed wind events in winter also occur at these two locations. However, their frequencies of occurrence are nearly an order of magnitude smaller than those for the northerly events and so they will not be considered in this study.

[11] Using the 15 m s^{-1} wind speed criterion noted above [see also *Moore and Renfrew*, 2005], we investigated the synoptic conditions associated with the high wind speed events. Events were identified during which this criterion was met. If this criterion was met more than once during a 72 hour long period, then the maximum wind speed during that period was used to define the time of the event. Other selection criteria returned similar results. Three different cases were considered: high speed wind events in November at the Cape Navarin site; high speed wind events in November at the Cape Olyutorsky site; and high speed wind events in February at the Cape Olyutorsky site. The sites selected were the locations of the maximum occurrence frequency during the months in question (Figure 1). In each of the three cases, approximately 100 events were identified over the 33 year period from 1979–2011, resulting in approximately 3 events per month for each case. Composites were created for the sea-level pressure field and the 10 m wind field.

[12] The composite for the November Cape Navarin case reveals that high speed winds at this site are associated with an extra-tropical cyclone centered over the central Bering Sea near 57°N, 175°W (Figure 3). Along the northwestern boundary of the Bering Sea, including the Gulf of Andayr, there is enhanced northeasterly flow with a 10 m wind speed maximum in excess of 17 m/s near Cape Navarin. In the lee of the headland, there is a region where the wind speed is reduced to approximately 10 m/s. The enhanced northeasterly flow is characterized by increased cross-isobar flow, especially in the vicinity of Cape Navarin. The monthly mean sea ice edge for November is included in Figure 3, but it has no discernable impact on the flow. The composite for the November Cape Olyutorsky case also shows enhanced northeasterly winds (Figure 4), but in this case the cyclone center is displaced to the southwest near 56°N, 172°E and the strongest flow, again in excess of 17 m/s, is near Cape Olyutorsky. Again there is a region of reduced wind speed in its lee as well as enhanced cross-isobar flow in its vicinity. The monthly mean sea ice can also be seen to have no impact on the flow.

[13] The corresponding composite for the February Cape Olyutorsky case is similar to that for the November case at this site, with an extra-tropical cyclone centered near 56°N, 172°E (Figure 5). However, the region of maximum wind speed is displaced eastwards by approximately 2° as expected from the similar offset in the location of the highest occurrence frequency during the two months (Figure 1). As a result of this offset, the region of reduced wind speed in the lee of the cape is not as pronounced. In addition, unlike the situation in November, the monthly sea ice edge can be seen to mark the boundary of the enhanced winds. Indeed,

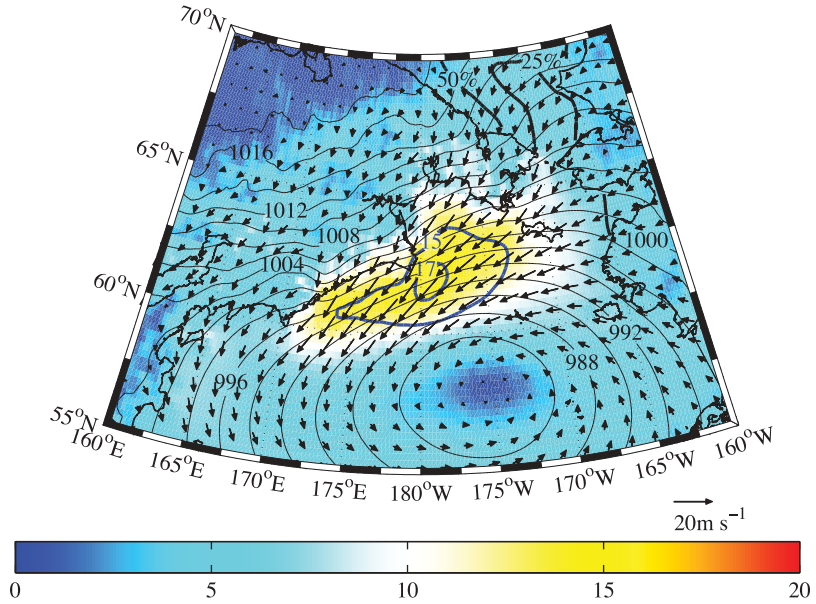

Figure 3. The composite 10 m wind field (m/s-vectors), its magnitude (m/s-shading) and the sea-level pressure field (mb-contours) for high speed wind events at the Cape Navarin site during November. Selected contours of the magnitude of the 10 m wind field are shown in blue. Also shown by the thick black lines are the monthly mean sea ice concentrations. Data from the NARR 1979–2011.

10 m wind speeds at Cape Navarin are approximately 50% smaller during the February Cape Olyutorsky composite as compared to that for November.

4. Discussion

[14] The Siberian coast of the northern Bering Sea has been identified as being the windiest location in the North Pacific region during the boreal winter [*Sampe and Xie*, 2007]. In this paper, we have identified intra-seasonal variability in the sites along this coast where high speed wind events are common. In particular, the two prominent headlands along this coast, Capes Navarin and Olyutorsky, each have a localized region where the occurrence frequency of high speed surface winds is elevated. In addition, the location of highest occurrence frequency at Cape Olyutorsky shifts offshore by approximately 100 km between November and February. At Cape Navarin, high speed wind events are

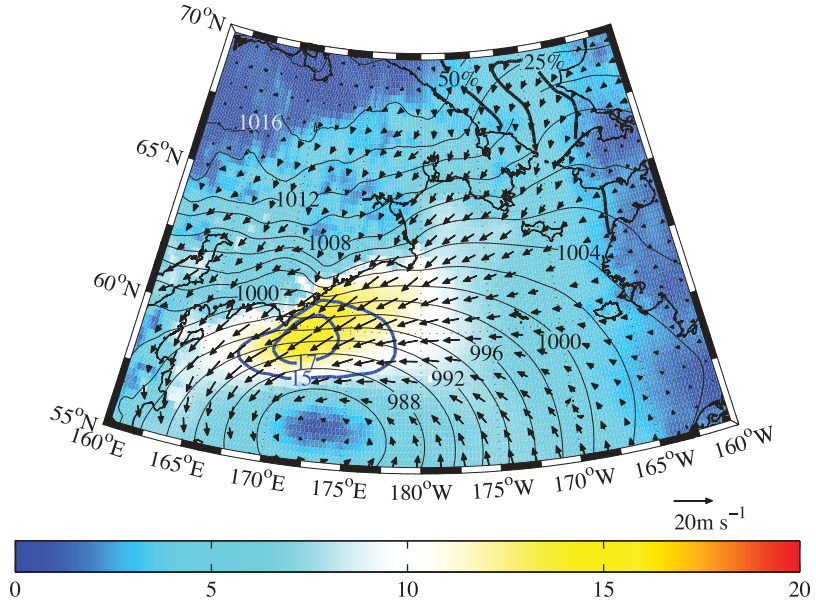

Figure 4. The composite 10 m wind field (m/s-vectors), its magnitude (m/s-shading) and the sea-level pressure field (mb-contours) for high speed wind events at the Cape Olyutorsky lsite during November. Selected contours of the magnitude of the 10 m wind field are shown in blue. Also shown by the thick black lines are the monthly mean sea ice concentrations. Data from the NARR 1979–2011.

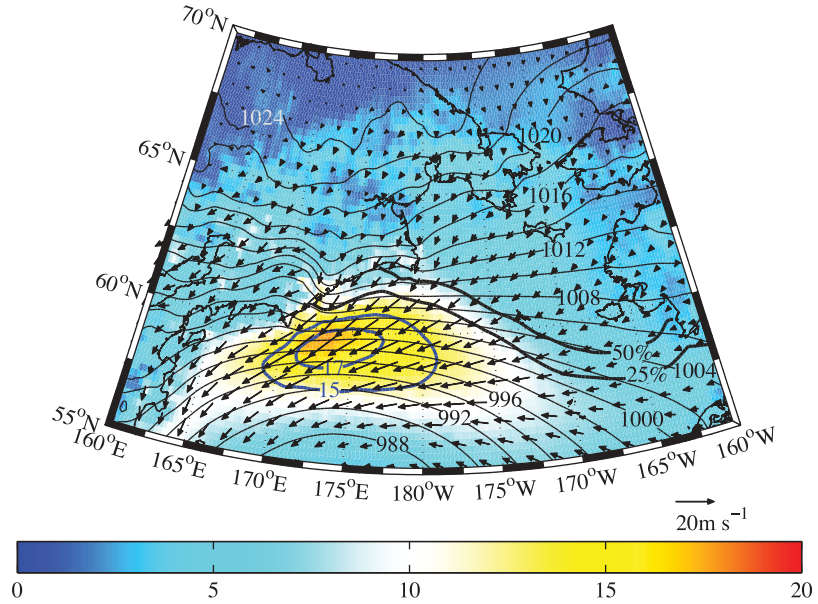

Figure 5. The composite 10 m wind field (m/s-vectors), its magnitude (m/s-shading) and the sea-level pressure field (mb-contours) for high speed wind events at the Cape Olyutorsky lsite during February. Selected contours of the magnitude of the 10 m wind field are shown in blue. Also shown by the thick black lines are the monthly mean sea ice concentrations. Data from the NARR 1979–2011.

most common during November–December; while at Cape Olyutorsky such events are common from November through March, with a maximum in February. The maximum occurrence frequency at the Cape Olyutorsky site (18%) is approximately 50% higher than that at the Cape Navarin site (11%).

[15] Since the capes are only 500 km apart, one might expect similar behavior at the two sites. Indeed, the composite high speed wind events at the two capes in November are quite similar. In particular, at each site the high speed winds are associated with the presence of an extra-tropical cyclone with a mean depth of approximately 986 mb to south of the site. In each case there is evidence of flow distortion in the vicinity of the respective cape, including cross-isobar flow, a wind speed maximum, and reduced wind speed in the lee of the cape. Although the situation in February at the Cape Olyutorsky site bears resemblance to the November composite, there are crucial differences. In particular, the evidence of flow distortion in the vicinity of the cape is more muted. In addition, the occurrence of the wind speed maximum is offset from the immediate vicinity of the cape.

[16] All of these differences can be attributed to the presence of sea ice in the vicinity of Cape Navarin during February. This leads to a deceleration of the surface winds due to increased roughness as compared to open water [*Petersen et al.*, 2009; *Pickart et al.*, 2009]. This is consistent with the observed reduction in winds over the sea ice as was seen during February (Figure 1b) as well as in the February composite (Figure 5). The absence of sea ice at Cape Navarin during the early winter, i.e., November–December, and its presence during the late winter, i.e., January to March, explains the early winter maximum occurrence frequency of high speed winds at this site and its rapid drop off in the following months (Figure 2). The encroachment of sea ice towards the Cape Olyutorsky site during the winter also explains the offshore shift in the location of the maximum in occurrence frequency (Figure 1). As the location shifts offshore, the jet loses some of the structure associated with flow distortion in the vicinity of the cape, and is instead subject to acceleration across the ice-edge due to the change in surface roughness. This behavior is similar to what has been observed in the southern Beaufort Sea [*Pickart et al.*, 2009]. In addition, the presence of a shallow boundary layer front along the ice edge may result in a low-level jet that would also result in a local acceleration of the wind [*Drue and Heinemann*, 2001].

[17] The composites of the high speed wind events during November (Figures 3 and 4) show evidence of flow distortion near the respective cape that is associated with cross-isobar acceleration to the left of the topographic barrier. As such, these tip jets are most likely examples of corner jets, a class of wind systems that include surface jets near Svalbard, Norway and easterly Cape Farewell tip jets [*Barstad and Gronas*, 2005; *Outten et al.*, 2009]. For example, the height of the topography and upstream conditions in the vicinity of the capes are similar to those in southern Norway where topographic flow distortion associated with corner jets occurs [*Barstad and Gronas*, 2005]. The presence of a region of reduced wind speed in the lee of the topography present in the November composites at both sites is also commonly seen in other corner jets [*Barstad and Gronas*, 2005; *Ohigashi and Moore*, 2009].

[18] There is also evidence of an inland elevated occurrence frequency of high speed wind events to the north of Cape Olyutorsky. From Figure S1, we note that this region is situated in the vicinity of Mt. Ledyakaya, which, with an elevation of 2400 m, is the highest point in the Koryak Mountains. It is likely that this region may experience gap flow as has been observed to occur over the Sea of Japan [*Sampe and Xie*, 2007].

[19] The atmospheric flow during each of the tip jet scenarios indicates that one would expect downwelling to occur

along the Siberian coast in the northern Bering Sea. In the Cape Navarin case this includes the Gulf of Anadyr, while in the Cape Olyutorsky case the downwelling would be more restricted to the region between the two capes. According to the numerical model study of *Wang et al.* [2009] the subsurface Anadyr current flows towards Bering Strait year-round, which is consistent with subsurface current meter data in Anadyr Strait [*Schumacher et al.*, 1983; *Muench et al.*, 1988]. This seems to suggest that the northeasterly tip jets are not able to completely reverse the Anadyr current, but weaken it [*Wang et al.*, 2009]. However, the wintertime polynya in the Gulf of Anadyr is one of the largest in the Bering and Chukchi Seas [*Cavalieri and Martin*, 1994], which implies that the surface currents in the northern Gulf readily advect ice offshore. This is consistent with the wintertime surface circulation in the *Wang et al.* [2009] numerical model. Furthermore, in the vicinity of Cape Navarin – where the tip jet is strongest – *Wang et al.*'s [2009] model shows that the inner portion of the Anadyr current does reverse to the south and is subject to downwelling of dense water. In light of the results presented here, more work is required to understand the time-dependent ocean response to the tip jets, including their impact on winter water formation and the subsequent transport of that dense water into Bering Strait and the Arctic Ocean. At present, many of the characteristics of the surface wind field presented in this study are not adequately represented in ocean circulation models forced by atmospheric fields that do not resolve the flow distortion in the region [*Wang et al.*, 2009].

[20] Finally, it is of interest to compare the tip jets revealed in this study with the more extensively investigated Cape Farewell tip jets. The synoptic Cape Farewell jets are embedded in an environment in which the mean winds are from the west and therefore the existence of both easterly and westerly jets is particularly striking and speaks to the difference in the dynamics between them. Although there also exist southerly high speed wind events along the Siberian coast, their occurrence frequency is much reduced, by an approximate order of magnitude, as compared to the northerly events. A common characteristic of both the Cape Farewell and Cape Navarin tip jets is that their formation involves the interaction of a low-pressure system with high topography. In both cases, there is strong evidence that these jets play an important role in forcing climatologically important oceanic circulations. Our identification of another region where flow distortion occurs as a result of cyclones interacting with coastal topography suggests that such small scale atmospheric phenomena may be common in other areas of the world ocean.

[21] **Acknowledgments.** The authors would like to thank the reviewers for their comments and the Physical Sciences Division of NOAA/ESRL for kindly providing access to their North American Regional Reanalysis data set. GWKM was supported by the Natural Science and Engineering Research Council of Canada. RSP was funded by grant NA08OAR43200895 from the National Oceanic and Atmospheric Administration.

[22] The Editor thanks the anonymous reviewer for assisting with the evaluation of this paper.

References

Barstad, I., and S. Gronas (2005), Southwesterly flows over southern Norway—Mesoscale sensitivity to large-scale wind direction and speed, *Tellus, Ser. A*, *57*, 136–152, doi:10.1111/j.1600-0870.2005.00112.x.

Cavalieri, D. J., and S. Martin (1994), The contribution of Alaskan, Siberian, and Canadian coastal polynyas to the cold halocline layer of the Arctic Ocean, *J. Geophys. Res.*, *99*, 18,343–18,362, doi:10.1029/94JC01169.

Doyle, J. D., and M. A. Shapiro (1999), Flow response to large-scale topography: The Greenland tip jet, *Tellus, Ser. A*, *51*, 728–748, doi:10.1034/j.1600-0870.1996.00014.x.

Drue, C., and G. Heinemann (2001), Airborne investigation of arctic boundary-layer fronts over the marginal ice zone of the Davis Strait, *Boundary Layer Meteorol.*, *101*, 261–292, doi:10.1023/A:1019223513815.

Haine, T. W. N., S. Zhang, G. W. K. Moore, and I. A. Renfrew (2009), On the impact of high-resolution, high-frequency meteorological forcing on Denmark Strait ocean circulation, *Q. J. R. Meteorol. Soc.*, *135*, 2067–2085, doi:10.1002/qj.505.

Highsmith, R. C., and K. O. Coyle (1990), High productivity of northern Bering Sea benthic amphipods, *Nature*, *344*, 862–864, doi:10.1038/344862a0.

Kanamaru, H., and M. Kanamitsu (2007), Fifty-seven-year California reanalysis downscaling at 10 km (CaRD10). Part II: Comparison with North American regional reanalysis, *J. Clim.*, *20*, 5572–5592, doi:10.1175/2007JCLI1522.1.

Mesinger, F., et al. (2006), North American regional reanalysis, *Bull. Am. Meteorol. Soc.*, *87*, 343–360, doi:10.1175/BAMS-87-3-343.

Moore, G. W. K. (2003), Gale force winds over the Irminger Sea to the east of Cape Farewell, Greenland, *Geophys. Res. Lett.*, *30*(17), 1894, doi:10.1029/2003GL018012.

Moore, G. W. K., and I. A. Renfrew (2005), Tip jets and barrier winds: A QuikSCAT climatology of high wind speed events around Greenland, *J. Clim.*, *18*, 3713–3725, doi:10.1175/JCLI3455.1.

Moore, G. W. K., R. S. Pickart, and I. A. Renfrew (2008), Buoy observations from the windiest location in the world ocean, Cape Farewell, Greenland, *Geophys. Res. Lett.*, *35*, L18802, doi:10.1029/2008GL034845.

Muench, R. D., J. D. Schumacher, and S. A. Salo (1988), Winter currents and hydrographic conditions on the northern central Bering Sea Shelf, *J. Geophys. Res.*, *93*(C1), 516–526, doi:10.1029/JC093iC01p00516.

New York Times (1999), 12 are missing after Japanese boat sinks, A4, 11 Dec.

Ohigashi, T., and G. W. K. Moore (2009), Fine structure of a Greenland reverse tip jet: A numerical simulation, *Tellus, Ser. A*, *61*, 512–526, doi:10.1111/j.1600-0870.2009.00399.x.

Outten, S. D., et al. (2009), An easterly tip jet off Cape Farewell, Greenland. II: Simulations and dynamics, *Q. J. R. Meteorol. Soc.*, *135*, 1934–1949, doi:10.1002/qj.531.

Petersen, G. N., et al. (2009), An overview of barrier winds off southeastern Greenland during the Greenland Flow Distortion experiment, *Q. J. R. Meteorol. Soc.*, *135*, 1950–1967, doi:10.1002/qj.455.

Pickart, R. S., et al. (2003), Deep convection in the Irminger Sea forced by the Greenland tip jet, *Nature*, *424*, 152–156, doi:10.1038/nature01729.

Pickart, R. S., G. W. K. Moore, D. J. Torres, P. S. Fratantoni, R. A. Goldsmith, and J. Yang (2009), Upwelling on the continental slope of the Alaskan Beaufort Sea: Storms, ice, and oceanographic response, *J. Geophys. Res.*, *114*, C00A13, doi:10.1029/2008JC005009.

Renfrew, I. A., et al. (2009a), An easterly tip jet off Cape Farewell, Greenland. I: Aircraft observations, *Q. J. R. Meteorol. Soc.*, *135*, 1919–1933, doi:10.1002/qj.513.

Renfrew, I. A., et al. (2009b), A comparison of aircraft-based surface-layer observations over Denmark Strait and the Irminger Sea with meteorological analyses and QuikSCAT winds, *Q. J. R. Meteorol. Soc.*, *135*, 2046–2066, doi:10.1002/qj.444.

Sampe, T., and S.-P. Xie (2007), Mapping high sea winds from space: A global climatology, *Bull. Am. Meteorol. Soc.*, *88*, 1965–1978, doi:10.1175/BAMS-88-12-1965.

Schumacher, J. D., K. Aagaard, C. H. Pease, and R. B. Tripp (1983), Effects of a shelf polynya on flow and water properties in the northern Bering Sea, *J. Geophys. Res.*, *88*, 2723–2732, doi:10.1029/JC088iC05p02723.

Våge, K., et al. (2009), Multi-event analysis of the westerly Greenland tip jet based upon 45 winters in ERA-40, *Q. J. R. Meteorol. Soc.*, *135*, 1999–2011, doi:10.1002/qj.488.

Wang, J., H. Hu, K. Mizobata, and S. Saitoh (2009), Seasonal variations of sea ice and ocean circulation in the Bering Sea: A model-data fusion study, *J. Geophys. Res.*, *114*, C02011, doi:10.1029/2008JC004727.